A Hybrid-learning Decomposition Algorithm for Competing Risk Identification within Fleets of Complex Engineering Systems

Hang Zhou *, Thiago Augusto Lopes Genez, Alexandra Brintrup, and Ajith Kumar Parlikad

There is an increasing interest in the reliability of complex engineering systems, especially in the systems' through-life risk analysis. A complex system, like the civil aircraft engine studied in this paper, contains multiple potential failure modes throughout its life that are contributed by various sub-system and component failures going through different deterioration processes. In order to fulfill the requirements of efficient swap and replacement maintenance strategies in the aviation industry, it is important to quantify the individual component risks within a complex system to enable an accurate prediction of spare parts demands. We propose a novel data-driven hybrid-learning algorithm with three building blocks: pre-defined reliability model based on the Weibull distribution, automated unsupervised clustering, and the quality check & output. The algorithm enables the identification of the riskiest sub-systems and the associated reliability models are quantitatively calculated.As all component risks follow the Weibull distribution, the parameters can be obtained. A case study carried out on a fleet of civil aircraft engines shows that the algorithm enables a better understanding of sub-system level risks from system level performance records, improving the efficient execution of the maintenance strategy.

I. Introduction

ONE of the fundamental tasks in reliability analysis is to develop a lifetime distribution model of systems using historical data on time-to-failure [1]–[5]. Such a model can then be used for predicting the remaining useful life (RUL) of a given system based on its operating age in the absence of other run-to-failure data. However, in most cases, complex systems fail due to several failure modes and the historical data often does not capture information about these failure modes separately [6], [7]. As the model is developed without due consideration of inherent failure modes, RUL prediction tends to be inaccurate.

Modern complex engineering systems tend to follow a modular design for efficient and cost-effective maintenance execution. For example, a civil aircraft engine, which is the targeted engineering asset in this paper, typically contains eight main modules: fan/low pressure compressor (LPC), intermediate pressure compressor (IPC), high pressure compressor (HPC), combustor (CBT), high pressure turbine (HPT), intermediate pressure turbine (IPT), low pressure turbine (LPT), and external gear box [8] as shown in Figure 1 [1]. The maintenance of aircraft engines, particularly the ones that are taken off-wing from airplanes and transported to maintenance facilities, are called overhauls. Overhauls are both necessary and costly. Therefore, the entire servicing requires careful and accurate planning. Effective planning of such overhauls is beneficial for both the engine manufacturer and its airline customers, as it minimizes the disturbance of flight operations. One key influential factor in guaranteeing the effectiveness of this maintenance strategy is sufficient availability of spare modules in any given time window. In order to accurately estimate the number and type of spares required, it is important to understand the performance patterns of the engine fleets with historical operational data, especially at the module level.

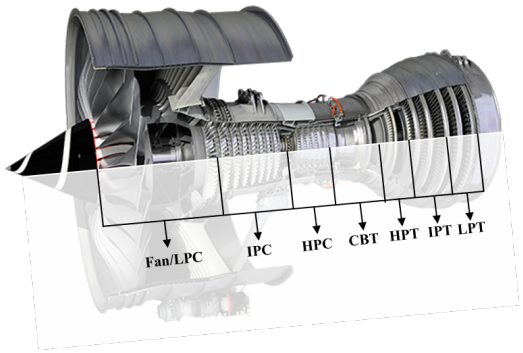

Fig. 1: Civil Aircraft Engine Module Overview

In the aviation industry, the failure information that causes each overhaul service is documented in engine-level maintenance logbooks. One of the practical challenges in extracting information is that actual records of engine removals in maintenance logbooks are in natural language, are complicated, and seldom clearly identify the module failures that necessitated

H.Zhou, T.A.L.Genez, A.Brintrup and A.K.Parlikad are with the Institute for Manufacturing, Department of Engineering, University of Cambridge, UK. * Correspondence e-mail: (hang.zhou@eng.cam.ac.uk).

This research is funded by the Aerospace Technology Institute (ATI) and InnovateUK

the overhaul. In most cases, the maintenance logbook states the primary reason for engine removal which is regarded as the root cause. However, there is normally no information on the condition of the other modules within the same engine, where even though failures happened due to other causes than the identified main root causes, this information is at times hidden. This leads to a common obstacle in real-life data processing where there is incomprehensive prior knowledge to the understanding of module-level failure information. We address this gap by proposing a novel technique for decomposition of sub-system level (module level) failure based on system level (engine level) failure data. This technique is founded on the principle of 'competing risks'.

The concept of competing risk applied in this paper is that single components and material within a complex system deteriorate at different speeds due to the different mechanical configurations and the environmental condition these components go through. At different periods of time, different types of failure dominate the failure reasons of the system. Especially when observing the complex engineering assets at a fleet level, particular issues in maintenance are concentrated at particular intervals during the life span of the system. We consider this phenomenon under the 'competing risks' framework, where the risks compete to be the root cause failures of the system.

The concept of 'competing risks' within a complex engineering system has been studied with different focuses. Sabri-Laghaie and Noorossana [9] define that the degradation in a complex system follows a Poisson process, which adds randomness to the failure of a system. They also propose that the reliability of a system is modeled with an exponential function. Cui et al. [10] propose two extended distributions to the classic N-phase-distribution. In Cui et al.'s research, the system is assumed as a Markov repairable system and the competing risks are classified as the 'emergency-state' decomposition at a system-level rather than individual risks at sub-system levels. Jiang [1] focused on the Poisson distribution and applied the analysis on bus-motor failure data. Jiang's research utilized a two-fold competing risk model where the risks are largely categorized as random failures and wear-out failures, not pointing at any specific sub-system of the bus motors. Similarly to Jiang's research, Wang and Pham [11] studied the dependent competing risk system with also two kinds of failure mechanism: the random shock failure and the degradation failure, on their influences to the perfect and imperfect maintenance policies. Further to these studies, recently there has been a growing research interest in dependent competing risks, where there are clear dependencies among sub-systems within a complex system [12]–[15]. In these studies both the statistical Bayesian non-parametric approach and the state-of-the-art deep reinforcement learning approach are applied in the estimation of component dependencies within a competing risk system. However, the civil aircraft engine design process seriously considers the possible dependencies among sub-systems, ensuring the failure of a component and sub-system does not cause the total failure of an engine, which may lead to catastrophic consequences. In fact, the engine system is designed to avoid dependencies in sub-systems. The study by Fang and Cui [16] tentatively examined the consideration of the multi-state competing risks where two parallel sub-systems are simulated to form a complex system, with the two sub-systems being of competing risks. In their study, the two sub-system risks are pre-defined, and the system is simpler than a system as complex as an aircraft engine, which contains at least eight main sub-systems. It is worth noting that there is a need for an effective algorithm to reveal quantified reliability estimation for sub-systems within an entire complex system.

The main challenge here is that there is a lack of available data where fleets of modular complex system are going through maintenance. Moreover, the root causes of such maintenance are due to multiple sub-system level failures. These challenges are addressed in our research where the civil aircraft engine maintenance logbooks contain both the information on run-to-failure service life for the entire data population and a limited amount of maintenance root causes at sub-system level. The maintenance logbooks support the necessary information.

In order to analyse the sub-system level reliability performance using competing risk decomposition, we propose an algorithm which is fundamentally a hybrid-learning approach: Due to the incomprehensive prior knowledge, it is essential to apply the unsupervised-learning clustering concept to group the data points that share similar properties. However, compared to some of the popular existing clustering algorithms where the similarity of data points within each cluster is based on the measurement of distance (K-means) [17], [18], fuzzy partition (Fuzzy C-means) [17] and distribution (Gaussian Mixture Model) [19], there is still a fundamental assumption as one pre-defined rule, which is that each module's probability of failure (PoF) follows the classic Weibull distribution reliability curve. The combination of the reliability model based on the Weibull distribution, along with the automated clustering

form the foundation of the hybrid-learning decomposition approach. The measurement of the fitness each datapoint belongs to one cluster is based on the distances between such points and the 'competing risk' Weibull reliability curve.

The hybrid-learning approach consists of three main building blocks. The Weibull distribution for reliability estimation is a classic approach in the field of reliability research and is continuously being studied to improve the accuracy and usability of Weibull models. The parameter estimation of the Weibull models is studied on block censored data in life testing of engineering products [20] and Type I censored data using the synthetic minority over-sampling technique [21], in order to obtain both the reliability model of the products and the accurate estimation of the product lives. Further research has also been carried out on the estimation of Weibull parameters for high quality products with zero-failure data, which is common in the industries with high reliability requirement, like the HDD industry [22]. The Weibull model is also the foundation for decisions of repair and maintenance strategies for complex engineering systems, where approaches including the Weibull-based regression model are used on repairable complex systems [23] and to describe the component degradation process [24]. The unsupervised approach of sub-system level failure case clustering is an effective way of extracting useful information when little prior-knowledge is obtained. The unsupervised-learning approach is an effective tool for sorting out the data for further processing and analysis, and has been applied successfully in many domains including to assist the improvement in depression treatment in the healthcare sector [25], to optimize the location of wind turbines in the energy industry [26], to identify the age of reclaimed asphalt binders in the construction industry [27], to perform dynamic risk assessment for the nuclear industry [28], to evaluate the fatigue damage equivalent load on a wind turbine blade in the aviation industry [29], and to optimize the maintenance strategy for a fleet of excavators in the mining industry [30]. Accordingly, clustering is one effective approach in discovering informative and valuable connections from collected data across multiple industries. However, a complex system is an integration of multiple sub-systems and components, and the failures occurring during the operations of such systems are often caused by a finite number of components within the system. This means that, upon the failure detection in a certain sub-system and component in the complex system, the majority of the system remains healthy and unharmed. The current studies observe the system as a single unit [23], or studies single component degradation without the association with the system level [24]. There is an obvious gap in understanding the performance and reliability of a complex system at multiple levels. The clustering approach introduced in this paper aims to bridge this gap.

The purpose of this paper is therefore to identify the sub-system level (module level) reliability curve from the system level (engine level) operational data based on the hybrid-learning approach by performing the competing risk analysis. This analysis will enable:

1) Improvement on planned maintenance (overhaul): An improved estimation of all the module demands at any given time window with better accuracy than simple estimation based on past experience.
2) Improvement on unplanned maintenance (overhaul): In order to generate the most value from each module, in the aviation industry the similar RUL modules can be re-assembled as an 'imperfect' engine for the most beneficial operation of each module before its retirement. In case the occurrence of unpredictable unplanned maintenance, the algorithm we propose in this paper provides the estimation of the RUL of the non-failure modules based on the modules' individual reliability curve.
3) Improvement in risky module demand prediction: In the aviation business operation, one of the major challenges is to have an accurate estimation of the risky module demands for unplanned maintenance. The proposed algorithm is dedicated to mitigate the occurrence of the costly unplanned maintenance and maintain the fleet with a high resilience. The algorithm enables statistical predictions of the demanded spare modules in any given time window, which leads to better planning in advance.

The proposed hybrid-learning algorithm also provides a benefit in utilizing the minimum amount of information on the competing risk detection of multi-module multi-failure-mode complex engineering system, with the purpose of improving both the performance of the planned and the unplanned maintenance.

The paper is organised as follows. In Section II, the methodology of the framework is described in detail. In Section III, a case study is provided, based on the dataset of a fleet the civil aircraft engine family provided by a our industrial research partner in the aviation industry, and the numerical results with the piecewise competing risk functions are given. A further real-life application of the algorithm is also provided

in Section III. In Section IV, we provide the conclusion and discuss the current limitations and the future work.

II. Failure Decomposition Methodology

This section describes the flow of the proposed algorithm.

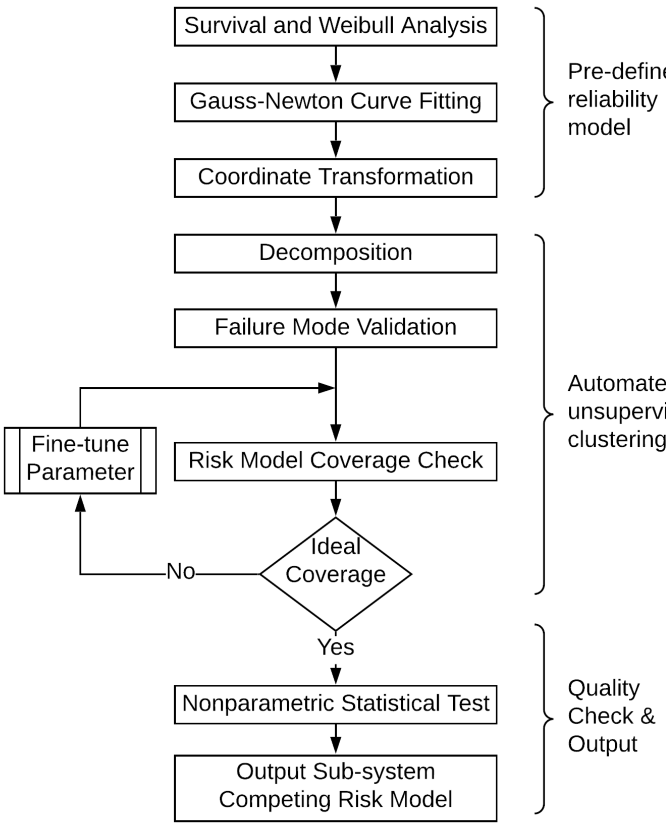

Fig. 2: Hybrid-learning decomposition algorithm

We assume that this analysis is being performed on a fleet of m identical assets. Each asset would have undergone a number of overhauls due to failures and the safe running duration before these failures occur is recorded for each asset. The input to the methodology consists of the total number of assets in the fleet and failure records over time. The proposed algorithm is illustrated in Figure 2.

As shown in Figure 2, the algorithm is divided into three main phases (building blocks):

1) The pre-defined reliability models: This step processes the maintenance data statistically and pre-defines that the failure models for both the civil aircraft engine at a system-level and each of the civil aircraft engine sub-system modules based on the Weibull distribution. The system-level recorded safe servicing life is processed via the survival analysis, fitted with Weibull analysis via the Gauss-Newton curve fitting and then being shifted in order to envelope the entire dataset for conservative and safety considerations (as the aviation industry has a high safety standard).
2) Automated unsupervised clustering: With the obtained system-level reliability model in Weibull format, the model goes through the autonomous differentiation in order to create sub-system Weibull models where the models cover the datapoints with similar root causes. The root causes of the datapoints validate the sub-system Weibull models on the efficacy of their descriptions of the sub-system competing risks. The efficacy of the model description is evaluated by the envelope coverage of such models, where the autonomous step is carried out until the satisfactory coverage rate is achieved.
3) Quality check & output: A further step ensuring the validity of the algorithm is carried out, which compares the unsupervised decomposition models with the observed failure cases from historical events. The comparison via the statistical tests supports the evidence that the decomposed risk model for sub-system modules well describes the observed samples, which leads to the output and application of such decomposed module risk models.

It is worth noting that this research discusses the statistical characteristics of the entire fleet, as a population, instead of any individual aircraft engine within the fleet. The target is also to solve the fleet maintenance planning, particularly the predictions of sub-system demands. Therefore, this research is in fact considering the non-ergodicity of each individual asset in the fleet.

These three phases are further described step by step as follows.

A. Pre-defined reliability models

We assume that system level PoF function is a superposition of sub-system level PoF functions. In other words, the system level PoF function is a continuous piece-wise function that is an envelope function of all the sub-system level PoF functions.

Step 1: Survival and Weibull analysis

The first step is to carry out Weibull analysis on the failure data. Let t_i be the time of the i^{th} asset failure.

Let d_i represent the total number of failed assets at time t_i. Let n_i be the number of assets that have been operating without a failure until time t_i. Although this is a well known procedure,

we articulate this here for clarity. The Kaplan-Meir estimator [31] for the survival function of the assets is given by:

$$\hat{S}(t_i) = \prod_{i:t_i \leq t_{max}} (1 - \frac{d_i}{n_i}) \tag{1}$$

The corresponding failure distribution is given by:

$$\hat{P}(t_i) = 1 - \prod_{i:t_i \leq t_{max}} (1 - \frac{d_i}{n_i}) \tag{2}$$

Here t_{max} is the maximum design life of a civil aircraft engine can reach with one maintenance interval. This analysis provides a tupple of engine performance $(t_i, \hat{P}(t_i))$ which is a datapoint within any mathematical coordinate system. The original cumulative density function of the Weibull distribution in a Cartesian coordinate system is:

$$F(t) = \int (\frac{k}{\lambda}(\frac{t}{\lambda})^{k-1} \mathrm{e}^{-(\frac{t}{\lambda})^k}) \, \mathrm{d}t = 1 - \mathrm{e}^{-(\frac{t}{\lambda})^k} \tag{3}$$

$F(t)$ the Weibull distribution function is the foundation for the logarithm transformation of the datapoints, it is worth noticing that in the variable t in $F(t)$ is continuous while the real values in the example datasets t_i are discrete data points within the domain. Taking logarithms on both side of equation (3) and rearranging, we get equation (4).

$$\ln \ln (\frac{1}{1 - F(t)}) = k \times \ln t - k \times \ln \lambda \tag{4}$$

The importance of performing the transformation shown in equation (4) is that under the new coordinate, a fitted linear function with a slope k and an intercept $c = (-k \times \ln \lambda)$ enables the determination of the two parameters on the Weibull reliability function. The x and y coordinates of the failure distribution function after the logarithm transformation is given by:

$$x_i(t_i) = \ln t_i \tag{5}$$

$$y_i(t_i) = \ln \ln \frac{1}{1 - \hat{P}(t_i)} = \ln \ln (\frac{1}{\prod_{i:t_i \leq t_{max}} (1 - \frac{d_i}{n_i})}) \tag{6}$$

The coordinate pairs (x_i, y_i) provides a mapping of the potential risk function.

Step 2: Gauss-Newton curve fitting

The purpose of this step is to obtain a function $f_I(x, \boldsymbol{\alpha_i})$, from a collection of I potential candidates of function formats, that fits the points obtained in step 1, where $\boldsymbol{\alpha_i}$ is a set of parameters $(\alpha_{i1}, \alpha_{i2}, \ldots, \alpha_{i\tau})$ of the function $f_I(x, \boldsymbol{\alpha_i})$ and $\tau < m$. Traditionally, a linear fit is performed on the data points. Since the objective here is to decompose the failure data to discover the different underlying failure modes, we take a different approach here.

In order to obtain the piecewise competing risk function, within the logarithm coordinate, the slope of each linear fitted competing risk function is required to be monotonically increasing. Assume a function $f_I(x)$ is fitted to the datapoints after logarithm transformation, where the derivative of the function $h_I(x) = \frac{df_I(x)}{dx}$ is monotonically increasing. Out of the common monotonically increasing functions, in this paper we choose three function formats which are monotonically increasing functions within the entire domain: the power function (linear polynomial), the exponential function and the logarithm function. Therefore we have:

$$\begin{cases} h_1(x) = a_{11} \ln x + a_{12} \\ h_2(x) = a_{21} e^x + a_{22} \\ h_3(x) = a_{31} x + a_{32} \end{cases} \tag{7}$$

Moreover, the choices of the first order derivatives $h_I(x)$ leads to the choices of potential fitting function for the datapoints after the logarithm transformation:

$$\begin{cases} f_1(x, \boldsymbol{\alpha_1}) = \int h_1(x) \, \mathrm{d}x = \alpha_{11} x \ln x + \alpha_{12} x + \alpha_{13} \\ f_2(x, \boldsymbol{\alpha_2}) = \int h_2(x) \, \mathrm{d}x = \alpha_{21} \mathrm{e}^x + \alpha_{22} x + \alpha_{23} \\ f_3(x, \boldsymbol{\alpha_3}) = \int h_3(x) \, \mathrm{d}x = \alpha_{31} x^2 + \alpha_{32} x + \alpha_{33} \end{cases} \tag{8}$$

In this paper, we have explored the use of the three potential functions listed in the set of equations (8). The transformed datapoints with their associated coordinates are fitted with an appropriate function using the non-linear least square (NLLS) [32] method. We have used the modified Gauss-Newton method [33], [34] for curve-fitting in this paper.

Each datapoint (x_i, y_i) has a residual r_i with respect to the fitted function:

$$r_i = y_i - f_I(x_i, \boldsymbol{\alpha_i}) \tag{9}$$

The function that best fits the data is obtained by minimizing the least squares of the residuals which is the sum of the residuals SR:

$$\operatorname{argmin} SR = \operatorname{argmin} (\sum_{i=1}^{m} r_i^2) \tag{10}$$

The minimum value of SR occurs when $\frac{\partial SR}{\partial \alpha_{i\tau}} = 2 \sum_i r_i \frac{\partial r_i}{\partial \alpha_{i\tau}} = 0$. With first order Taylor expansion the potential choices of monotonic functions:

$$\begin{aligned} f_I(x_i, \boldsymbol{\alpha_i}) \approx & f_I(x_i, \boldsymbol{\alpha_i}^{\boldsymbol{k}}) + \sum_{\tau} \frac{\partial f_I(x_i, \boldsymbol{\alpha_i}^{\boldsymbol{k}})}{\partial \alpha_{i\tau}} (\alpha_{i\tau} - {\alpha_{i\tau}}^k) \\ = & f_I(x_i, \boldsymbol{\alpha_i}^{\boldsymbol{k}}) + \sum_{\tau} \boldsymbol{J_I} \Delta \alpha_{i\tau} \end{aligned} \tag{11}$$

where the notation $\boldsymbol{k}$ represents the k^{th} iteration of undetermined parameters of the algorithm, and $\boldsymbol{J_I}$ is the Jacobian of the function $f_I(x_i, \boldsymbol{\alpha_i})$.

Let

$$\begin{cases} \Delta y_i = y_i - f_I(x_i, \boldsymbol{\alpha_i}^{\boldsymbol{k}}) \\ r_i = (y_i - f_I(x_i, \boldsymbol{\alpha_i}^{\boldsymbol{k}})) + (f_I(x_i, \boldsymbol{\alpha_i}^{\boldsymbol{k}}) - f_I(x_i, \boldsymbol{\alpha_i})) \\ \qquad \approx \Delta y_i - \sum_{\tau} \boldsymbol{J_I} \Delta \alpha_{i\tau} \end{cases} \tag{12}$$

From equation (12) it can be concluded that

$$(\boldsymbol{J}^T \boldsymbol{J}) \Delta \boldsymbol{\alpha} = \boldsymbol{J}^T \Delta y \tag{13}$$

The iteration value achieves optimality when increments in parameter matrix $\boldsymbol{\alpha}$ do not lead to any obvious increment in the objective value of y.

The required calculation in the curve fitting step is the Jacobians of all the potential functions which are obvious:

$$\begin{cases} \boldsymbol{J_1} = [x \ln x \quad x \quad 1]^T \\ \boldsymbol{J_2} = [e^x \quad x \quad 1]^T \\ \boldsymbol{J_3} = [x^2 \quad x \quad 1]^T \end{cases} \tag{14}$$

Step 2 therefore identifies the set of parameters $\boldsymbol{\alpha_1} = [\alpha_{11}\ \alpha_{12}\ \alpha_{13}]$, $\boldsymbol{\alpha_2} = [\alpha_{21}\ \alpha_{22}\ \alpha_{23}]$, and $\boldsymbol{\alpha_3} = [\alpha_{31}\ \alpha_{32}\ \alpha_{33}]$ for each of the potential functions for their best fit to the survival analysis datapoints. The function that describes the recorded datapoints the best is taken further to Step 3 for coordinate transformation. The choice of the best function $f_I(x, \alpha_i)$ will be in the next step denoted by $f(x, \alpha)$.

Step 3: Coordinate transformation

The function obtained from Step 3 is the function that obtains the trend of the datapoints. However, since each datapoint represents an actual failure case, there will be points where $f(x_i, \boldsymbol{\alpha})$ is less than or greater than y_i.

When considering the reliability of complex engineering systems in certain safety-critical industries such as the aviation industry, it is important that the estimated failure distribution function cover the majority of the failure cases, or in another word, it is optimum that the reliability function is an envelope function to all the recorded datapoints in any mathematical coordinate system. As the datasets in this research are records of real failure cases for civil aircraft engine overhauls, none of the recorded datapoints are treated as outliers or noise. Hence the functions with the optimized parameters in step 2 need to be shifted in order to envelope the decent amount of recorded failure cases. This amount, measured by a percentage of failure cases Ω, is the trade-off risk threshold an industry can accept. As the failure cases not enveloped by the function shifting cause discrepancies in the next step of automated sub-system probability of failure decomposition, and further influence maintenance planning. The threshold is normally determined by the industrial end-users of this algorithm. It is worth noticing that the risk threshold step is optional is based on the risk-appetite of the organization.

Under such a requirement, the coordinate transformation presented in this step should be performed on the fitted function, which aims to keep the shape of the fitted function, but shifts it so that the new function envelopes all the existing (historical) datapoints. The procedure for obtaining this shifted envelope function is presented in Algorithm 1.

Algorithm 1 Coordinate transformation with risk threshold

procedure CURVE-SHIFT
  for $i \leftarrow 1, m$ **do**
    $[d_{y_i}] \leftarrow [y_i - f(x_i, \boldsymbol{\alpha})]$ ▷ data shift y-axis
  end for
  $\boldsymbol{D_y} \leftarrow [d_{y_1}, d_{y_2} ... d_{y_m}]$ ▷ array of distances
  $\boldsymbol{D_y}' \leftarrow [d_{y_1}', d_{y_2}' ... d_{y_m}']$ ▷ sort $\min_i \boldsymbol{D_y} \rightarrow \max_i \boldsymbol{D_y}$
  $m' \leftarrow m \times (1 - \Omega)$ ▷ risk acceptance threshold
  $\boldsymbol{D_y}'' \leftarrow [d_{y_1}', d_{y_2}' ... d_{y_{m-m'}}']$
  $\vec{Y} \leftarrow (0, \max_i \boldsymbol{D_y}'')$ ▷ minimum y shift
  for $i \leftarrow 1, m$ **do**
    solve $f(x_i', \boldsymbol{\alpha}) = y_i$
    obtain x_i'
    $[d_{x_i}] \leftarrow [x_i - x_i']$ ▷ data shift x-axis
  end for
  $\boldsymbol{D_x} \leftarrow [d_{x_1}, d_{x_2} ... d_{x_m}]$ ▷ array of distances x-axis
  $\boldsymbol{D_x}' \leftarrow [d_{x_1}', d_{x_2}' ... d_{x_m}']$ ▷ sort $\max_i \boldsymbol{D_x} \rightarrow \min_i \boldsymbol{D_x}$
  $\boldsymbol{D_x}'' \leftarrow [d_{x_1}', d_{x_2}' ... d_{x_{m-m'}}']$
  $\vec{X} \leftarrow (0, \min_i \boldsymbol{D_x}'')$ ▷ minimum x shift
  $LS_x \leftarrow \sum_{i=1}^{m} f(x_i + |\min_i \boldsymbol{D_x}''|, \boldsymbol{\alpha}) - y_i$
  $LS_y \leftarrow \sum_{i=1}^{m} f(x_i, \boldsymbol{\alpha}) - y_i + |\max_i \boldsymbol{D_y}''|$
  $C \leftarrow LS_x - LS_y$ ▷ discriminant for shift direction
  if $C \geq 0$ **then**
    $F(x) \leftarrow f(x) + \max_i \boldsymbol{D_y}''$
  else
    $F(x) \leftarrow f(x + \min_i \boldsymbol{D_x}'')$
  end if
  return $F(x)$ ▷ The shifted envelope function is $F(x)$
end procedure

B. Automated unsupervised clustering

The purpose of this phase is to generate the competing risk models for the most risky sub-system modules within the

logarithm coordinate.

Step 4: Decomposition

Now, we need to obtain the piece-wise failure distribution for each part of the decomposition. Here, we introduce the concept of *winning risk function*, which is defined as the failure distribution function that represents the failure that contributes to the maintenance action at a given time. Consider the module swapping maintenance strategy for the civil aircraft engines. It is possible to identify the hierarchy of sub-system modules within the engine when maintenance is required, based on the time this engine has been used. The health conditions of the top risky modules are estimated by this algorithm, at any time point maintenance activities are required.

Algorithm 2 presents the approach for decomposing the enveloped function $F(x)$ into its competing risk functions within the logarithm coordinate. With incomprehensive prior knowledge of engine module failures, this algorithm is fundamentally an automated clustering step where the datapoints within the logarithm coordinate are clustered according to their distances to the decomposed sub-system level reliability functions.

Algorithm 2 Automated decomposition clustering

```
procedure DECOMPOSE
    j, r, i ← 1
    while r < m do
        while j < m do
            k[j] ← dF(x)/dx |_{x=x_j}          ▷ slope at x = x_j
            c[j] ← F(x_j) − k[j]x_j            ▷ intercept at x = x_i
            g_r(x) ← k[j]x + c[j]              ▷ r^th risk function
            while i < m do
                δ_i ← g_r(x_i) − y_i
                if δ_i < 0 then                ▷ check if enveloped
                    j ← i
                    r ← r + 1
                    BREAK
                elseif i ≡ m and δ_i ≥ 0
                    end all loop
                end if
            end while
        end while
    end while
end procedure
```

The explanation of the algorithm is as follows. Starting from the first data point (x_1, y_1) the derivative of the envelope function $F(x)$ is obtained at $(x_1, F(x_1))$, which is given by $\frac{dF(x)}{dx}\Big|_{x=x_1}$. The intercept of the related linear function is $F(x_1) - \frac{dF(x)}{dx}\Big|_{x=x_1} x_1$. The first linear function within the logarithm coordinate is therefore given by:

$$g_1(x) = \frac{dF(x)}{dx}\Big|_{x=x_1} x_1 + F(x_1) - \frac{dF(x)}{dx}\Big|_{x=x_1} x_1 \quad (15)$$

The above equation is the first competing risk function and the first piecewise function describing the probability of failure of one sub-system module. Moving on to the second failure data point (x_2, y_2), we study whether each data point is enveloped by the first risk function, by calculating the distance of datapoint (x_2, y_2) to the first competing risk function $\delta_2 = g_1(x_2) - y_2$. If $\delta_2 \geq 0$, it is considered that the previous risk function is still the competing risk for the second recorded failure case. This iteration continues until $\delta_q < 0$, which means that the q^{th} data point is the start of another competing risk different from the previous competing risk. A new differentiation is then performed at (x_q, y_q), obtaining the new competing risk function as:

$$g_r(x) = \frac{dF(x)}{dx}\Big|_{x=x_{q_r}} x_{q_r} + F(x_{q_r}) - \frac{dF(x)}{dx}\Big|_{x=x_{q_r}} x_{q_r} \quad (16)$$

Here, $g_r(x)$ is the r^{th} piecewise competing risk function. The iteration is performed until the last failure data point (x_m, y_m).

This Algorithm 2 completes the automated clustering of datapoints in a logarithm coordinate under the presumed reliability models based on Weibull distribution, the cluster results automatically provide the risk functions at a sub-system level from the maintenance information at the system-level. In this step, one competing risk function points to one identified sub-system module failure. When a datapoint is above the previous risk function, it is likely that the system has moved towards another phase of operation, while another category of failure modes pointing at another sub-system module is taking over as the sub-system module with a higher failure probability. This, however, does not rule out the other sub-system modules with other failure modes from happening simultaneously with the sub-system module possessing the highest failure probability. The other sub-systems are with a lower hierarchical failure probability ranking within each maintenance time window.

Note that the competing risk functions obtained in step 4 using the the Algorithm 2 are in logarithmic coordinates.

Step 5: Failure mode validation with risk function parameter fine-tune

Automated unsupervised clustering is an allocation of initial competing risk models to sub-system modules within an entire system. The Algorithm 2 in Step 4 has the capability of decomposing a system level dataset to $3-6$ sub-system competing risk models. An important step here is to validate

the effectiveness of the initial sub-system module risk models. Often within a given maintenance record dataset, there are root causes of a maintenance activity being carried out, pointing at failure modes in one of the sub-system modules. However, due to the imperfectness of any real-life dataset, there is constantly the situation of missing records, or the records are not sufficiently informative to identify the exact causes. Furthermore, with the concept introduced in this research, the root causes of the maintenance activities always targets the most observable sub-system module at the time point. However, other sub-systems may have also suffered from part failures without being identified when making the maintenance decision. This consideration is interpreted as: the observed failure datapoints of any sub-system module are independently drafted samples from the general risk model of this sub-system module.

The initial deduced competing risk models are then compared with the observed sub-system module failure datapoints, to determine the effectiveness of the decomposition algorithm. The effectiveness is defined as the coverage rate of the competing risk model towards the observed draft failure datapoints. An ideal coverage of the datapoints by the linear competing risk model in the logarithm coordinate means the risk model can effectively predict the failure of such sub-system module. The coverage rate $R_c = \frac{CoveredFailureCases}{TotalFailureCases}$ should pass a threshold $\boldsymbol{R}$. On the occasion that the initial competing risk model does not reach the coverage threshold $\boldsymbol{R}$, the parameters of the initial competing risk function is required to be 'fine-tuned' in order to reasonably describe the observed failure cases. The parameter fine-tuning algorithm is explained in Algorithm 3.

Assume there is a set of j observed failure sample $\boldsymbol{S_{M_i}} = \{S_{M_{i_1}}, S_{M_{i_2}}, ..., S_{M_{i_j}}\}$, pointing at the same sub-system module M_i, where the observed samples are considered as independently drafted and extracted from the system-level failure data. The location of this set of samples in the logarithm coordinate is $\boldsymbol{L_{M_i}} = \begin{bmatrix} x_{M_{i_1}} & x_{M_{i_2}} & ... & x_{M_{i_l}} \\ y_{M_{i_1}} & y_{M_{i_2}} & ... & y_{M_{i_l}} \end{bmatrix}$, where $\boldsymbol{L_{M_i}}$ is a $2 \times l$ matrix for the coordinates of all the observed samples.

The output risk models towards the top risky sub-system modules from the fine-tuning step is thus the reasonable risk models that can describe the population of the drafted samples. Therefore, the automated clustering of datapoints with fine-tuned parameters of the outputs is accomplished with the analytic geometry calculations. The output functions after 'parameter fine-tuning' replace the original functions, and the notation of these functions and parameters remain the same, with replaced values.

Algorithm 3 Parameter fine-tuning

procedure FINE-TUNING
  $k_{initial} \leftarrow k_{tune} \leftarrow \frac{dF(x)}{dx}\Big|_{x=x_{q_r}}$
  $m_{initial} \leftarrow m_{tune} \leftarrow F(x_{q_r}) - \frac{dF(x)}{dx}\Big|_{x=x_{q_r}} x_{q_r}$
  for $\xi \leftarrow 1, l$ **do**
    for $\rho \leftarrow 1, l$ **do**
      if $g_r(\boldsymbol{L_{M_i}}_{1,\rho}) - \boldsymbol{L_{M_i}}_{2,\rho} \geq 0$ **then**
        $Count_{cover} \leftarrow Count_{cover} + 1$
      else if $g_r(\boldsymbol{L_{m_i}}_{1,\rho}) - \boldsymbol{L_{M_i}}_{2,\rho} < 0$ **then**
        $Count_{uncover} \leftarrow Count_{uncover} + 1$
      end if
      $R_c \leftarrow \frac{Count_{cover}}{Count_{cover}+Count_{uncover}}$ ▷ Coverage Rate
    end for
    if $R_c < \boldsymbol{R}$ **then** ▷ Coverage Threshold
      $k_{tune} \leftarrow \frac{dF(x)}{dx}\Big|_{x=L_{M_i 1,\xi}}$
      $m_{tune} \leftarrow F(L_{M_i 1,\xi}) - k_{tune} \times L_{M_i 1,\xi}$
      $g_r \leftarrow g_r[k_{tune}, m_{tune}]$ ▷ fine-tune g_r
    else if $R_c \geq \boldsymbol{R}$ **then**
      BREAK
    end if
  end for
end procedure

C. Quality check & output

The third and the final phase of the proposed algorithm is the quality check and output of the competing risk models in the Cartesian coordinate.

Step 6: Nonparametric statistical test

The purpose of this step is to ensure that the linear competing risk models in the logarithm coordinate is not of significant statistical differences from the observed sub-system level failure cases. With the condition that the assumed risk models are fulfilling the Weibull distribution and there is no comprehensive prior knowledge of the distribution of the independently observed failure cases, the nonparametric statistical test is used to justify the output risk models. Assume one of the output risk models describing one sub-system module, and the referenced recorded sub-system module failure cases are from two independent sample sets, the Mann-Whitney U test [35] is used for the examination. The set of ψ observed failure sample $\boldsymbol{S_{m_i}} = \{S_{m_{i_1}}, S_{m_{i_2}}, ..., S_{m_{i_p}}\}$ for sub-system m_i, is compared with the ω independently drafted samples $i.i.d\ \boldsymbol{G} = \{g_r{}'(x_1), g_r{}'(x_2), ..., g_r{}'(x_q)\}$ from the competing risk model $g_r(x)$. The U statistics is calculated by rank-sum:

$$U = \sum_{p=1}^{\psi} \sum_{q=1}^{\omega} M(S_{m_{i_p}}, g_r{}'(x_q)) \tag{17}$$

where

$$M(\boldsymbol{S_{m_i}}, \boldsymbol{G}) = \begin{cases} 1, if\ \boldsymbol{G} < \boldsymbol{S_{m_i}} \\ \frac{1}{2}, if\ \boldsymbol{G} = \boldsymbol{S_{m_i}} \\ 0, if\ \boldsymbol{G} > \boldsymbol{S_{m_i}} \end{cases} \tag{18}$$

For relatively large observation sample size, the sum of ranks for both samples are obtained:

$$\begin{cases} U_1 = R_1 - \frac{\psi(\psi+1)}{2} \\ U_2 = R_2 - \frac{\omega(\omega+1)}{2} \end{cases} \tag{19}$$

U_1 is the U statistics calculated by equation (18) for sample 1, where R_1 is the sum of ranks for sample 1. Similarly R_2 is the sum of ranks for sample 2.

$$U = min\{U_1, U_2\} \tag{20}$$

The null hypothesis is further checked for validity by the Mann-Whitney Table [36]. Once the test is passed, meaning the competing risk model and the observed failure datapoints on sub-systems are not of significance difference, the models are further carried on towards the next step.

Step 7: Weibull parameter calculation for sub-system competing risk model output

In the previous step, the competing risk functions obtained are within the logarithm coordinate system, the final step of the proposed algorithm is to transfer the deducted competing risks back from the logarithm coordinate system to the Cartesian coordinate system. One typical competing risk function from Step 4 with the linear slope of $\frac{dF(x)}{dx}\Big|_{x=x_{q_r}}$, the slope value obtained in the logarithm coordinate system is the shape parameter k of the Weibull distribution in the Cartesian coordinate system.

$$\frac{dF(x)}{dx}\Big|_{x=x_{q_r}} = k_r \tag{21}$$

The intercept of the linear risk function in the logarithm coordinate system is given by:

$$F(x_{q_r}) - \frac{dF(x)}{dx}\Big|_{x=x_{q_r}} x_{q_r} = -k_r \times \ln \lambda_r \tag{22}$$

This relationship is used to calculate the scale parameter of the Weibull distribution in the Cartesian coordinate system as follows:

$$\lambda_r = \exp\left(- \frac{F(x_{q_r}) - \frac{dF(x)}{dx}\Big|_{x=x_{q_r}} x_{q_r}}{\frac{dF(x)}{dx}\Big|_{x=x_{q_r}}} \right) \tag{23}$$

This leads to the r^{th} competing risk function in the Cartesian coordinate system as follows:

$$RF_r(t) = 1 - \exp\left(- \left(\frac{t}{\exp\left(- \frac{F(x_{q_r}) - \frac{dF(x)}{dx}\Big|_{x=x_{q_r}} x_{q_r}}{\frac{dF(x)}{dx}\Big|_{x=x_{q_r}}} \right)} \right)^{\frac{dF(x)}{dx}\Big|_{x=x_{q_r}}} \right) \tag{24}$$

III. Case example

A. Results of hybrid-learning competing risk analysis

The example is based on real performance data provided by a major aircraft engine manufacturer and maintenance service provider. The data consists of 327 recorded maintenance cases across a fleet belonging to the same family of engines operated by different airlines. These maintenance cases are specifically unplanned overhaul maintenance instead of suspension maintenance, meaning a failure symptom clearly exists and is observed when the decision of overhaul is made.

Model	Label	Operator	Service (hrs)	Root Cause
1	2168	OP51	485673	IPC OGV CRACKING
1	2731	OP71	719590	HPC VANE DAMAGE
1	1788	OP32	7752774	HPT BLADE THERMAL E
1	1456	OP5	10870557	LPT BEARING
1	2248	OP20	12332413	HPC SURGE MARGIN
⋮	⋮	⋮	⋮	⋮

TABLE I: Excerpt of aircraft engine failure data

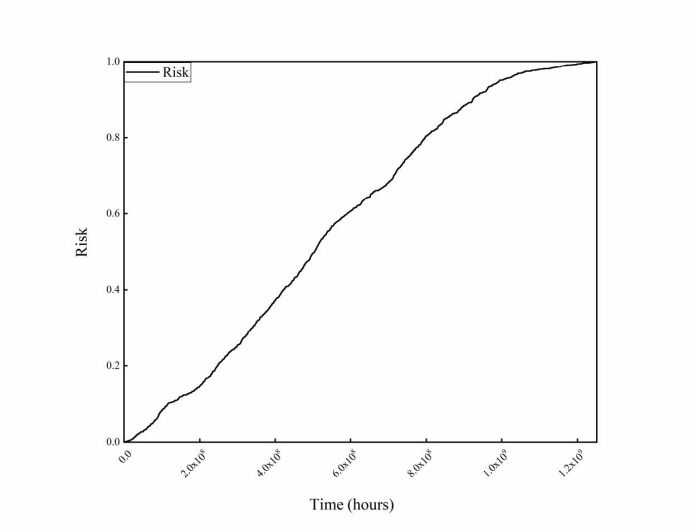

(a) Actual data

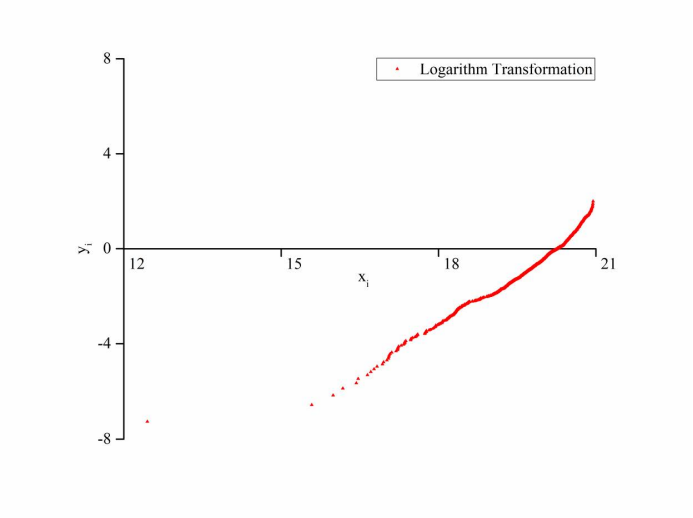

(b) Logarithm coordinates

Fig. 3: Civil aircraft engine family risk and logarithm transformation

In Table I, the first column refers to the specific model of the engine. The second column refers to the specific engine within the fleet. The third column refers to the customer (airline) that the specific engine belongs to. The fourth column refers to the life consumption of engine in service before a maintenance activity is taken place. All the maintenance activities in this research are off-wing overhauls with engine removal, the on-wing maintenance at airports are not included nor considered in this research. And the last column states the short description of root causes of the engine removals and decision of overhauls. It is worth noticing that for confidential reasons, the fourth column values are scaled from the exact value. This, however, does not influence the effectiveness of the proposed algorithm in this paper as all the values are scaled with the same proportional factor.

1) Results of Phase 1

Following step 1, first of all, the collected unplanned shop visit overhaul data of the engine family fleet is performed the survival analysis and the Weibull analysis, and the result is shown in Figure 3.

Figure 3(a) shows the survival analysis distribution of the aircraft engine service lives before overhauls. Figure 3(b) shows the risk plot after the logarithmic transformation. Moving to steps 2 and 3 of the methodology, the best function to describe the data points within the logarithm coordinate is selected. The mean squared error (MSE) of the three choices of function formats are shown in Table II.

Target Function	MSE
Logarithm Function	0.005482
Quadratic Function	0.004707
Exponential Function	0.004647

TABLE II: Selection of Best Fit Function in Logarithm Coordinate

It can be observed that, for the dataset being discussed in this use-case, the exponential function is the best choice with the minimum MSE colored in red. However, the differences among the three function choices is marginal, meaning a different dataset has the opportunity to end up with a different selection of function format. The exponential function format is further discussed as the choice for this use case study in this section.

The envelope function of the datapoints with the consideration of risk acceptance threshold is identified and is shown in Fig. 4

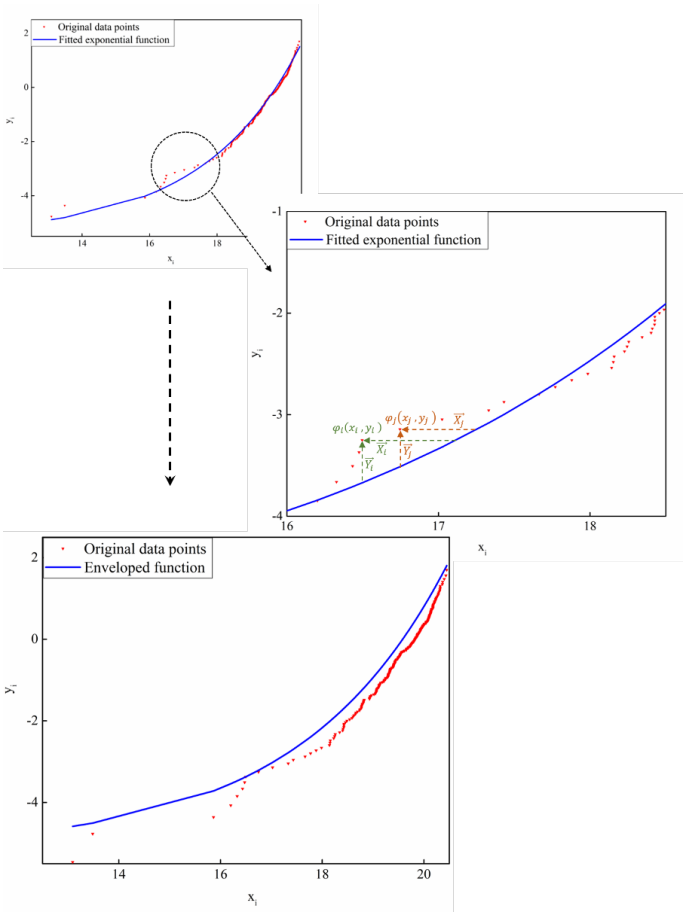

Fig. 4: Envelope risk function for the engine family

Here the function $\varphi(x, y)$ represents the combination of distances that the fitted function need to shift in order to envelope the specific datapoint. As can be seen in Figure 4, the fitted function does not envelope all failure cases, which might result in excessive risks for the organisation. In Algorithm 1, there is a pre-defined risk acceptance threshold Ω, this influences the shift of the function in order to cover the population of the recorded failure data. Due to the study is focused on the aviation industry, specifically the civil aircraft engine, the demand of reliability is extremely high. Therefore, the risk acceptance threshold set up in this study is $\Omega = 99.5\%$. The shift of the fitted function in order to envelope all the failure datapoints also provides a marginal higher estimation of PoF at any time point. This is particularly important for the aviation industry for the trade-off of maintenance. Simultaneously, the best fitted function with the minimum possible shift from Algorithm 1 guarantees the aircraft engine to fly more hours and use up the available healthy life as much as possible. With this consideration, we obtain the envelope function with an exponential function format: $\frac{df(x)}{dx} = 8.9832 \times 10^{-10} e^x + 1.3948x - 28.3548$.

2) Results of Phase 2

After obtaining the envelope risk function, Algorithm 2 from step 4 is performed on the envelope risk function to obtain the decomposed competing risk functions, which four linear functions that are decomposed from the original envelope risk function. This matches the top four most frequently observed sub-system module failures from the aircraft engine family studied in this research. The top four highest risky modules, the number of failure observations within this engine family and the main failure mechanism are listed in Table III.

Module	Sample NO	Main Failure Mode
IPC	38	OGV Blade Cracking
HPC	36	Compressor Surge Blade Damage
HPT	22	Turbine Blade Holing Damage
FAN/LPC	19	Corrosion

TABLE III: Top Risky Sub-system Modules and Main Failure Modes

The locations of the observed samples for four modules within the logarithm coordinate are compared with the initial output of the competing risk models before fully accepting them, following step 5.During the process of the second building block, automated unsupervised clustering process, only one competing model, the competing risk model 1 requires the Algorithm 3 in step 5 - parameter fine-tuning. The target of the coverage rate R_c for each competing risk model is 90% This competing risk model, pointing at the HPC failure, initially with a coverage rate of $\frac{30}{38}$, required a further two iterations of Algorithm 3 to achieve the coverage rate $R_c = \frac{36}{38} = 94.7\%$. The coverage rates of the four competing risk models towards four aircraft engine modules after Algorithm 3 are shown in Table IV. The decomposition results are also shown in Figure 5. The figure shows the original data points, the envelope risk function and its decomposed linear functions.

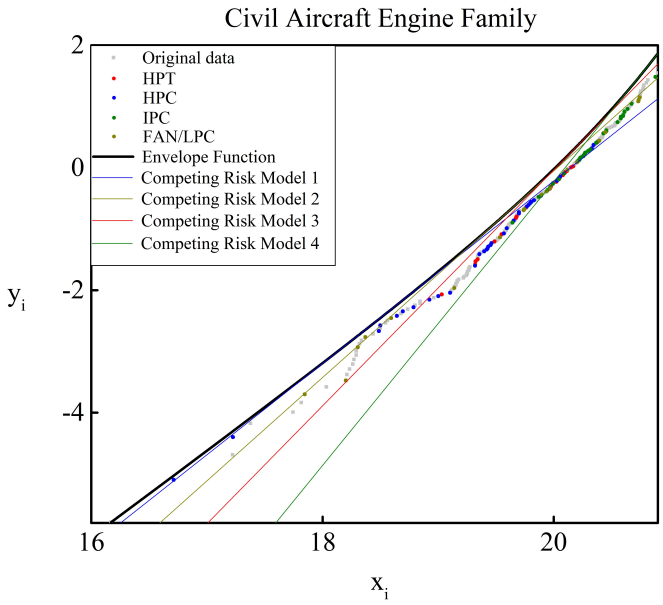

Fig. 5: Competing risk function in logarithm coordinates

In Figure 5, the black line represents the envelope function after curve shifting. The blue line is the competing risk model 1 for HPC module. The yellow line is the competing risk model 2 for FAN/LPC module. The red line is the competing risk model 3 for HPT module. And the green line is the competing risk model 4 for the IPC module. The first two phases enabled decomposition of the entire system failure data into four sub-system module competing risk models. This is reasonable as fundamentally not all modules within an aircraft engine possess the same useful life and are of the same level of risk during operations. The algorithm identified the top four risk modules and the related competing risk models. The fact that after the initial decomposition, only one competing risk model required parameter fine-tuning and this specific step was accomplished by 2 iterations proves the effectiveness of the algorithm.

Competing Risk Model	Coverage Rate R_c
1	94.4%
2	94.7%
3	95.5%
4	94.7%

TABLE IV: Coverage rate R_c for competing risk models

The confirmed slope and intercept parameters of the linear competing risk models within the logarithm coordinate are shown in Table V.

3) Results of Phase 3

Before the competing risk models are converted from the logarithm linear functions to the Weibull models in the Cartesian coordinate, the Mann-Whitney U test is performed on all the risk models and observed module failure samples to ensure the models' capability of describing the independently drafted observations.

Model	Module	Slope k	Interception m
1	HPC	1.4908	-30.0301
2	FAN/LPC	1.6880	-33.8096
3	HPT	1.9271	-38.5752
4	IPC	2.3183	-46.5948

TABLE V: Linear Competing Risk Model Parameters in Logarithm Coordinate

To ensure the randomness of the 'observed sample' (Sample 1) and the 'sample extracted from the competing risk model' (Sample 2), the competing risk sample size is always linked to the sample size of the observed sample size. In this study, the Mann-Whitney U test is performed on the comparison of the entire sample size of Sample 1 and half the size of Sample 1 for Sample 2, on all four aircraft engine modules. The null hypothesis H_0 is that there is no evidence of significant differences between the competing risk model and the observed failure samples. To further enhance the effectiveness of the nonparametric statistical test, the U statistics value are calculated based on the average of 20 independent iterations, and is recorded as $U_{average}$. The comparison results are shown in Table 6:

Module	Sample 1	Sample 2	$U_{average}$	U_{limit}
HPC	36	18	193.8	173
FAN/LPC	19	9	64.2	29
HPT	22	11	61.2	49
IPC	38	19	209.1	197

TABLE VI: Mann-Whitney U Test on Competing Risk Model and Observed Failure Samples

In Table VI, it can be observed that all the U statistics values $U_{average}$ shown in red are larger than the U_{limit} values for $Alpha = 0.05$ of two-tailed test referring to the Mann-Whitney U test table. This result supports the null hypothesis H_0 and suggests that the hypothesis is not likely to be rejected, which means the competing risks has no significant differences than the observed failure samples for all the four modules. Hence it can be concluded that the competing risk model can describe the module failure cases well.

This further lead to the resulting Weibull cumulative distribution functions (CDF) representing the competing risks in each time window are shown in Figure 6. The Weibull parameters, the shape parameter K and the scale parameter λ for all the four competing risk models are shown in Table VII.

Model	Module	Shape K	Scale λ
1	HPC	1.4908	5.6006×10^8
2	FAN/LPC	1.6880	4.9963×10^8
3	HPT	1.9271	4.9354×10^8
4	IPC	2.3183	5.3549×10^8

TABLE VII: Weibull Competing Risk Model Parameters in Cartesian Coordinate

This provides the following competing risk functions for the four high risk modules:

$$\begin{cases} CR_{1HPC} = 1 - \mathrm{e}^{-(\frac{t}{5.6006\times10^8})^{1.4908}} \\ CR_{2FAN/LPC} = 1 - \mathrm{e}^{-(\frac{t}{4.9963\times10^8})^{1.688}} \\ CR_{3HPT} = 1 - \mathrm{e}^{-(\frac{t}{4.9354\times10^8})^{1.9271}} \\ CR_{4IPC} = 1 - \mathrm{e}^{-(\frac{t}{5.3549\times10^8})^{2.3183}} \end{cases}$$

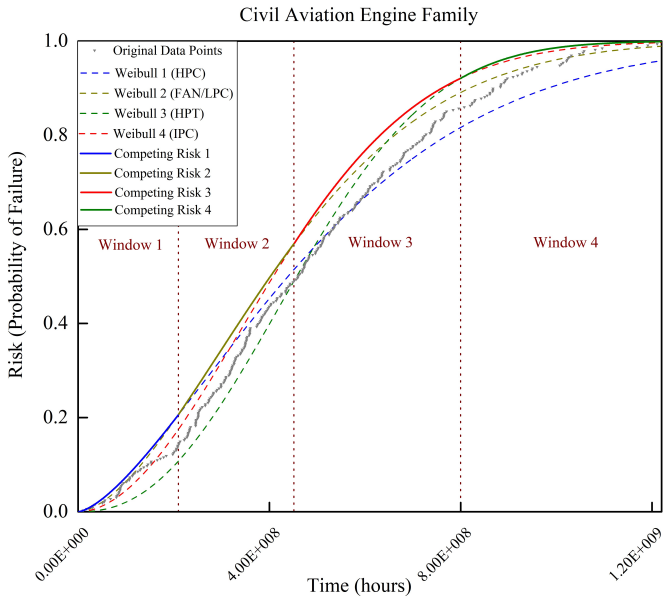

Fig. 6: Decomposed Weibull failure CDFs of the competing risks

Figure 6 showcases the four competing risk models of the four most risky modules in this aircraft engine family. The four competing risks take the 'winning' failure root causes in turn and creates four time windows for the fleet performance descriptions of this engine family. The reliability of the entire engine family population is further described by the outer boundaries of the four competing risk models, in solid line plots. The dashed lines represent the continuous probability of failure for each module. Within certain time window, these dashed lines are not the 'winning competing risks' of the engine removal and overhaul, which means they are not the observations inspected initially for the engine failure. But there is still a probability that these modules suffer deterioration, and should be prioritised for maintenance when engines are shipped to overhaul facilities. The four competing risk models are named CR_I.

B. Application - Module Demand Prediction

The rationale for the module swapping maintenance strategy used by the engine manufacturer is the efficiency in getting the engines back to the airline operators. The key target of the engine manufacturer is to cause the minimum disturbance to airlines, ensuring the maximum available flying hours within an engine's life-cycle. The efficiency of module swapping is dependant on the availability of demanded modules when engine-removal occurs. Hence it is important to have an accurate estimation of modules to be stocked as inventory in warehouses within the overhaul facilities. A difficulty in estimating demand for such modules is the occurrence of unplanned maintenance, as the trade-off for module demand is the adequate availability at any time window and limitations in storage capacities.

The algorithm proposed in this paper focuses on the module failure decomposition of the unplanned maintenance data, and is particularly useful in providing insights for the estimation of high risky module demands in any future time interval.

Figure 7 shows the estimate of module demands for time interval Δt as deduced from the competing risk functions. The red star marks indicate the likelihood of demand for each of the high risk modules when predicting from the current engine flying status t_i towards a future status $t_i + \Delta t$. The current status t_i could denote the age of the engine is flying from new or the time from the last overhaul when the engine was refurbished to its 100% healthy status.

Consider an airline owning a fleet of n engines from the studied engine family, each flying at a status $t_i, i = 1, 2, ..., n$. The demand prediction D_κ where $\kappa = 1, 2, 3, \&4$ for the four high risk modules given a prediction time interval Δt is:

$$\begin{cases} D_1 = \sum_{i=1}^{n} CR_1(t_i + \Delta t) \\ D_2 = \sum_{i=1}^{n} CR_2(t_i + \Delta t) \\ D_3 = \sum_{i=1}^{n} CR_3(t_i + \Delta t) \\ D_4 = \sum_{i=1}^{n} CR_4(t_i + \Delta t) \end{cases}$$

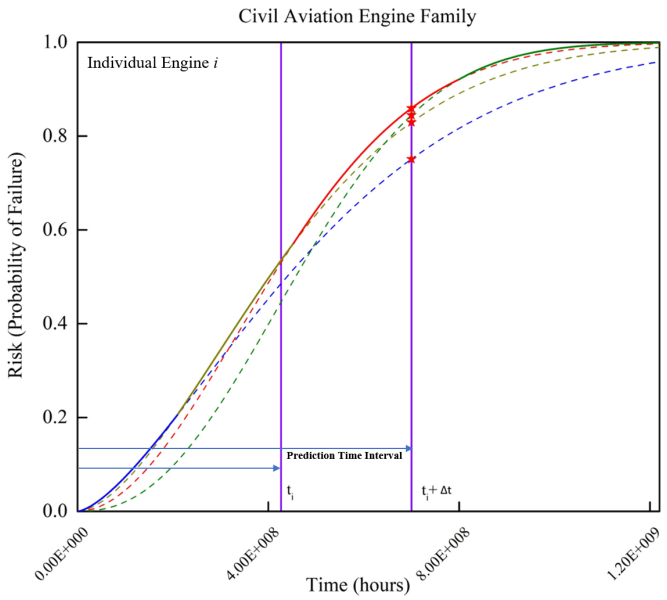

Fig. 7: Module Demand Likelihood for Engine i for a Given Prediction Time Interval

A numerical example is provided, where a small sized airline possess a fleet of 50 pairs of engines (50 aircrafts) from the studied engine family. Each pair of engines flying at the same status t_i from the purchase or from the last full overhaul refurbishment. The target is the prediction of demanded high risky modules in the next 1×10^8 flying hours. The current status values and the future status values are shown in the Appendix. The predicted demand for the four modules are:

$$\begin{cases} D_{1HPC} = \sum_{i=1}^{50} CR_1(t_i + 1 \times 10^8) \times 2 \approx 42 \\ D_{2FAN/LPC} = \sum_{i=1}^{50} CR_2(t_i + 1 \times 10^8) \times 2 \approx 46 \\ D_{3HPT} = \sum_{i=1}^{50} CR_3(t_i + 1 \times 10^8) \times 2 \approx 44 \\ D_{4IPC} = \sum_{i=1}^{50} CR_4(t_i + 1 \times 10^8) \times 2 \approx 38 \end{cases}$$

The prediction time interval fully considers the lead time for these modules from manufacturing to shipping for a guaranteed availability in case of unplanned maintenance. Considering airline structures with a larger fleet of aircrafts, the possession of multiple models of aircrafts with different engine families, the age of the fleets (young fleet or aged fleet), etc., the algorithm proposed in this paper with the algorithm building blocks is highly valuable for the service insights, the health monitoring and the maintenance planning activities. This approach is beneficial for both the system maintenance service providers and the system end-users.

IV. Conclusion

This paper presented a novel framework for the decomposition of potential failure modes of a complex engineering system. This approach allows the manufacturer, maintenance service provider and end-users of complex systems to achieve maximum usage of simple historical failure data to discover the potential risks within any specific fleet of systems.

Conventionally, in mechanical industrial applications, the failure data is analysed by a fitted Weibull distribution [37]. The difficulty of this method arises when the data points do not fit well by the control of the two input parameters (i.e. shape and scale). Especially for application domains where a conservative approach needs to be taken, no failure data should be disregarded from the risk model, which the Weibull approach cannot adequately address.

The decomposition algorithm we propose provides a trade-off between not fully using the asset value and the control of risks. Statistically recognising a certain number of winning risk causes within the fleet provides a closer fit of piecewise risk functions, as well as being conservative, and therefore suits the philosophy of the industries that are risk-conservative. It is especially valuable when insufficient prior knowledge is available to identify the exact sub-system level risks.

With the algorithm as well as the case study we aim to provide insights for the aviation industry on the reliability uncertainties in maintenance planning. The unplanned maintenance is one of the most costly situations in fleet management, particularly when key components/sub-systems are not available. The proposed algorithm with its ability to automatically identify the high risky sub-systems and quantified probability of failure of the associated sub-systems fills the uncertainty space, also statistically improves the understanding of assets reliability on unexpected events. The output of the algorithm provides a means to perform maintenance activity planning, particularly providing a service insight for the demand of parts and sub-systems where unplanned maintenance regularly happens. This enhances the parts and module availability in urgent scenarios, providing values for both the maintenance service providers and the engineering system end-users.

The limitation of this approach discussed in the paper is the available data size. Since we are studying the real life data obtained throughout the past decades, it is effective, valuable and accurate on the engine models That have entered the market with a considerable duration of servicing history. It is still a challenge for newly developed engine models to utilise the approach in this paper where much fewer maintenance records are so far documented.

In future work, further enhancement to our approach will include consideration of the more detailed component level. Additionally, the maintenance planning on multiple indepen-

dent parallel and seires sub-systems within a complex system is also of great interest. The authors are further working on the topics of maintenance strategies of multi-component, multi-sub-system maintenance policies and optimization, as well as the influence of fleet resilience on executing such policies.

ACKNOWLEDGMENT

This research was funded by Aerospace Technology Institute and Innovate UK through the TES-Digital (113174) project.

REFERENCES

[1] P. Jiang, J.-H. Lim, M. J. Zuo, and B. Guo, "Reliability estimation in a Weibull lifetime distribution with zero-failure field data," *Quality and Reliability Engineering International*, vol. 26, no. 7, pp. 691–701, Nov. 2010, ISSN: 0748-8017. DOI: 10.1002/qre.1138. [Online]. Available: https://doi.org/10.1002/qre.1138.

[2] H.-Z. Huang, C. Ping-Liang, P. Weiwen, G. Hui-Ying, and W. Hai-Kun, *Fatigue Lifetime Assessment of Aircraft Engine Disc via Multi-source Information Fusion*, 2014. DOI: 10.1515/tjj-2013-0043. [Online]. Available: https://www.degruyter.com/view/j/tjj.2014.31.issue-2/tjj-2013-0043/tjj-2013-0043.xml.

[3] H. Zhao and A. A. Tsiatis, "Estimating Mean Quality Adjusted Lifetime with Censored Data," *Sankhyā: The Indian Journal of Statistics, Series B (1960-2002)*, vol. 62, no. 1, pp. 175–188, Feb. 2000, ISSN: 05815738. [Online]. Available: http://www.jstor.org/stable/25053126.

[4] B. Pradhan and D. Kundu, "Analysis of Interval-Censored Data with Weibull Lifetime Distribution," *Sankhyā: The Indian Journal of Statistics, Series B (2008-)*, vol. 76, no. 1, pp. 120–139, Feb. 2014, ISSN: 09768386, 09768394. [Online]. Available: http://www.jstor.org/stable/43694408.

[5] P. Wouters, A. van Schijndel, and J. M. Wetzer, "Remaining lifetime modeling of power transformers: individual assets and fleets," *IEEE Electrical Insulation Magazine*, vol. 27, 2011.

[6] J. E. HUNT, D. R. PUGH, and C. J. PRICE, "FAILURE MODE EFFECTS ANALYSIS: A PRACTICAL APPLICATION OF FUNCTIONAL MODELING," *Applied Artificial Intelligence*, vol. 9, no. 1, pp. 33–44, Jan. 1995, ISSN: 0883-9514. DOI: 10.1080/08839519508945466. [Online]. Available: https://doi.org/10.1080/08839519508945466.

[7] J. Mi, Y.-F. Li, W. Peng, and H.-Z. Huang, "Reliability analysis of complex multi-state system with common cause failure based on evidential networks," *Reliability Engineering & System Safety*, vol. 174, pp. 71–81, 2018, ISSN: 0951-8320. DOI: https://doi.org/10.1016/j.ress.2018.02.021. [Online]. Available: http://www.sciencedirect.com/science/article/pii/S0951832016309553.

[8] S. Ackert, "Engine maintenance concepts for financiers - elements of turbofan shop maintenance costs," 2011.

[9] K. Sabri-Laghaie and R. Noorossana, "Reliability and maintenance models for a competing-risk system subjected to random usage," *IEEE Transactions on Reliability*, vol. 65, no. 3, pp. 1271–1283, 2016. DOI: 10.1109/TR.2016.2570574.

[10] L. Cui and B. Wu, "Extended phase-type models for multistate competing risk systems," *Reliability Engineering System Safety*, vol. 181, pp. 1–16, 2019, ISSN: 0951-8320. DOI: https://doi.org/10.1016/j.ress.2018.08.015. [Online]. Available: http://www.sciencedirect.com/science/article/pii/S0951832018302643.

[11] Y. Wang and H. Pham, "A multi-objective optimization of imperfect preventive maintenance policy for dependent competing risk systems with hidden failure," *IEEE Transactions on Reliability*, vol. 60, no. 4, pp. 770–781, 2011. DOI: 10.1109/TR.2011.2167779.

[12] M. P. Almeida, R. S. Paixão, P. L. Ramos, V. Tomazella, F. Louzada, and R. S. Ehlers, "Bayesian non-parametric frailty model for dependent competing risks in a repairable systems framework," *Reliability Engineering System Safety*, vol. 204, p. 107 145, 2020, ISSN: 0951-8320. DOI: https://doi.org/10.1016/j.ress.2020.107145. [Online]. Available: https://www.sciencedirect.com/science/article/pii/S0951832020306463.

[13] N. Zhang and W. Si, "Deep reinforcement learning for condition-based maintenance planning of multi-component systems under dependent competing risks," *Reliability Engineering System Safety*, vol. 203, p. 107 094, 2020, ISSN: 0951-8320. DOI: https://doi.org/10.1016/j.ress.2020.107094. [Online]. Available: https://www.sciencedirect.com/science/article/pii/S0951832020305950.

[14] J. Wang, Z. Li, G. Bai, and M. J. Zuo, "An improved model for dependent competing risks considering continuous degradation and random shocks," *Reliability Engineering System Safety*, vol. 193, p. 106 641, 2020, ISSN: 0951-8320. DOI: https://doi.org/10.1016/j.ress.2019.106641. [Online]. Available: https://www.sciencedirect.com/science/article/pii/S0951832017310414.

[15] B. Liu, Y. Shi, H. K. T. Ng, and X. Shang, "Nonparametric bayesian reliability analysis of masked data with dependent competing risks," *Reliability Engineering System Safety*, vol. 210, p. 107 502, 2021, ISSN: 0951-8320. DOI: https://doi.org/10.1016/j.ress.2021.107502. [Online]. Available: https://www.sciencedirect.com/science/article/pii/S095183202100065X.

[16] C. Fang and L. Cui, "Balanced systems by considering multi-state competing risks under degradation processes," *Reliability Engineering System Safety*, vol. 205, p. 107 252, 2021, ISSN: 0951-8320. DOI: https://doi.org/10.1016/j.ress.2020.107252. [Online]. Available: https://www.sciencedirect.com/science/article/pii/S0951832020307523.

[17] T. Warren Liao, "Clustering of time series data—a survey," *Pattern Recognition*, vol. 38, no. 11, pp. 1857–1874, 2005, ISSN: 0031-3203. DOI: https://doi.org/10.1016/j.patcog.2005.01.025.

[18] R. C. de Amorim and C. Hennig, "Recovering the number of clusters in data sets with noise features using feature rescaling factors," *Information Sciences*, vol. 324, pp. 126–145, 2015, ISSN: 0020-0255. DOI: https://doi.org/10.1016/j.ins.2015.06.039.

[19] P. Hedelin and J. Skoglund, "Vector quantization based on gaussian mixture models," *IEEE Transactions on Speech and Audio Processing*, vol. 8, no. 4, pp. 385–401, 2000, ISSN: 1558-2353. DOI: 10.1109/89.848220.

[20] T. Zhu, "Reliability estimation for two-parameter weibull distribution under block censoring," *Reliability Engineering System Safety*, vol. 203, p. 107 071, 2020, ISSN: 0951-8320. DOI: https://doi.org/10.1016/j.ress.2020.107071. [Online]. Available: https://www.sciencedirect.com/science/article/pii/S095183202030572X.

[21] J. K. Starling, C. Mastrangelo, and Y. Choe, "Improving weibull distribution estimation for generalized type i censored data using modified smote," *Reliability Engineering System Safety*, vol. 211, p. 107 505, 2021, ISSN: 0951-8320. DOI: https://doi.org/10.1016/j.ress.2021.107505. [Online]. Available: https://www.sciencedirect.com/science/article/pii/S0951832021000661.

[22] C. W. Zhang, "Weibull parameter estimation and reliability analysis with zero-failure data from high-quality products," *Reliability Engineering System Safety*, vol. 207, p. 107 321, 2021, ISSN: 0951-8320. DOI: https://doi.org/10.1016/j.ress.2020.107321. [Online]. Available: https://www.sciencedirect.com/science/article/pii/S0951832020308140.

[23] W. Hu, Z. Yang, C. Chen, Y. Wu, and Q. Xie, "A weibull-based recurrent regression model for repairable systems considering double effects of operation and

maintenance: A case study of machine tools," *Reliability Engineering System Safety*, p. 107 669, 2021, ISSN: 0951-8320. DOI: https://doi.org/10.1016/j.ress.2021.107669. [Online]. Available: https://www.sciencedirect.com/science/article/pii/S095183202100209X.

[24] M. Compare, P. Baraldi, I. Bani, E. Zio, and D. McDonnell, "Industrial equipment reliability estimation: A bayesian weibull regression model with covariate selection," *Reliability Engineering System Safety*, vol. 200, p. 106 891, 2020, ISSN: 0951-8320. DOI: https://doi.org/10.1016/j.ress.2020.106891. [Online]. Available: https://www.sciencedirect.com/science/article/pii/S0951832019300481.

[25] A. J. Dietrich, T. E. Oxman, J. W. Williams, H. C. Schulberg, M. L. Bruce, P. W. Lee, S. Barry, P. J. Raue, J. J. Lefever, M. Heo, K. Rost, K. Kroenke, M. Gerrity, and P. A. Nutting, "Re-engineering systems for the treatment of depression in primary care: Cluster randomised controlled trial," *BMJ*, vol. 329, no. 7466, p. 602, 2004, ISSN: 0959-8138. DOI: 10.1136/bmj.38219.481250.55. eprint: https://www.bmj.com/content/329/7466/602.full.pdf. [Online]. Available: https://www.bmj.com/content/329/7466/602.

[26] C. Zhang, X. Lu, G. Ren, S. Chen, C. Hu, Z. Kong, N. Zhang, and A. M. Foley, "Optimal allocation of onshore wind power in china based on cluster analysis," *Applied Energy*, vol. 285, p. 116 482, 2021, ISSN: 0306-2619. DOI: https://doi.org/10.1016/j.apenergy.2021.116482. [Online]. Available: https://www.sciencedirect.com/science/article/pii/S0306261921000453.

[27] A. Margaritis, H. Soenen, E. Fransen, G. Pipintakos, G. Jacobs, J. Blom, and W. Van den bergh, "Identification of ageing state clusters of reclaimed asphalt binders using principal component analysis (pca) and hierarchical cluster analysis (hca) based on chemo-rheological parameters," *Construction and Building Materials*, vol. 244, p. 118 276, 2020, ISSN: 0950-0618. DOI: https://doi.org/10.1016/j.conbuildmat.2020.118276. [Online]. Available: https://www.sciencedirect.com/science/article/pii/S0950061820302816.

[28] J. Kim, A. U. A. Shah, and H. G. Kang, "Dynamic risk assessment with bayesian network and clustering analysis," *Reliability Engineering System Safety*, vol. 201, p. 106 959, 2020, ISSN: 0951-8320. DOI: https://doi.org/10.1016/j.ress.2020.106959. [Online]. Available: https://www.sciencedirect.com/science/article/pii/S095183201931035X.

[29] I. Abdallah, K. Tatsis, and E. Chatzi, "Unsupervised local cluster-weighted bootstrap aggregating the output from multiple stochastic simulators," *Reliability Engineering System Safety*, vol. 199, p. 106 876, 2020, ISSN: 0951-8320. DOI: https://doi.org/10.1016/j.ress.2020.106876. [Online]. Available: https://www.sciencedirect.com/science/article/pii/S0951832019303096.

[30] Z. Yang, P. Baraldi, and E. Zio, "A novel method for maintenance record clustering and its application to a case study of maintenance optimization," *Reliability Engineering System Safety*, vol. 203, p. 107 103, 2020, ISSN: 0951-8320. DOI: https://doi.org/10.1016/j.ress.2020.107103. [Online]. Available: https://www.sciencedirect.com/science/article/pii/S0951832020306049.

[31] E. L. Kaplan and P. Meier, "Nonparametric Estimation from Incomplete Observations," *Journal of the American Statistical Association*, vol. 53, no. 282, pp. 457–481, Feb. 1958, ISSN: 01621459. DOI: 10.2307/2281868. [Online]. Available: http://www.jstor.org/stable/2281868.

[32] M. Gan, C. L. P. Chen, G. Chen, and L. Chen, "On some separated algorithms for separable nonlinear least squares problems," *IEEE Transactions on Cybernetics*, vol. 48, no. 10, pp. 2866–2874, Oct. 2018, ISSN: 2168-2275. DOI: 10.1109/TCYB.2017.2751558.

[33] Á. A. Magreñán and I. K. Argyros, *Chapter 7 - Proximal Gauss–Newton method*, Á. A. Magreñán and I. K. B. T. A. C. S. o. I. M. Argyros, Eds., 2018. DOI: https://doi.org/10.1016/B978-0-12-809214-9.00007-3. [Online]. Available: http://www.sciencedirect.com/science/article/pii/B9780128092149000073.

[34] M. Meloun and J. Militký, *8 - Nonlinear Regression Models*, M. Meloun and J. B. T. S. D. A. Militký, Eds., 2011. DOI: https://doi.org/10.1533/9780857097200.667. [Online]. Available: http://www.sciencedirect.com/science/article/pii/B978085709109350008X.

[35] T. W. MacFarland and J. M. Yates, "Mann–whitney u test," in *Introduction to Nonparametric Statistics for the Biological Sciences Using R*. Cham: Springer International Publishing, 2016, pp. 103–132, ISBN: 978-3-319-30634-6. DOI: 10.1007/978-3-319-30634-6_4. [Online]. Available: https://doi.org/10.1007/978-3-319-30634-6_4.

[36] "Appendix 1: Statistical tables," in *Experimental Design and Statistics for Psychology*. John Wiley Sons, Ltd, 2006, pp. 183–196, ISBN: 9780470776124. DOI: https : / / doi . org / 10 . 1002 / 9780470776124 . app1. eprint: https : / / onlinelibrary . wiley . com / doi / pdf / 10 . 1002 / 9780470776124 . app1. [Online]. Available: https : / / onlinelibrary . wiley . com / doi / abs / 10 . 1002 / 9780470776124.app1.

[37] R. Abernethy, J. Breneman, C. Medlin, and G. Reinman, "Weibull Analysis Handbook," p. 243, Nov. 1983.

APPENDIX

Engine i	Flying Status (Flying Hour)	Future Status (With Time Interval)
1	5.58385e+08	6.58385e+08
2	4.67327e+08	5.67327e+08
3	2.14363e+08	3.14363e+08
4	4.32801e+08	5.32801e+08
5	2.90867e+08	3.90867e+08
6	1.06598e+08	2.06598e+08
7	4.59087e+07	1.45909e+08
8	2.4127e+08	3.4127e+08
9	3.76432e+08	4.76432e+08
10	2.97297e+08	3.97297e+08
11	3.57536e+08	4.57536e+08
12	4.56805e+08	5.56805e+08
13	1.17504e+08	2.17504e+08
14	5.25919e+08	6.25919e+08
15	1.36218e+08	2.36218e+08
16	1.58386e+08	2.58386e+08
17	1.80671e+07	1.18067e+08
18	3.57729e+07	1.35773e+08
19	2.74453e+08	3.74453e+08
20	4.68481e+08	5.68481e+08
21	5.20875e+08	6.20875e+08
22	1.13857e+08	2.13857e+08
23	2.78262e+08	3.78262e+08
24	4.42859e+08	5.42859e+08
25	3.0787e+08	4.0787e+08
26	3.02401e+08	4.02401e+08
27	4.98286e+07	1.49829e+08
28	1.64708e+08	2.64708e+08
29	2.93179e+07	1.29318e+08
30	1.00701e+08	2.00701e+08
31	4.96543e+07	1.49654e+08
32	1.78994e+08	2.78994e+08
33	3.2456e+08	4.2456e+08
34	3.7977e+08	4.7977e+08
35	1.6215e+08	2.6215e+08
36	3.00615e+08	4.00615e+08
37	1.22252e+08	2.22252e+08
38	5.92684e+07	1.59268e+08
39	3.11393e+08	4.11393e+08
40	5.84062e+08	6.84062e+08
41	5.96542e+08	6.96542e+08
42	3.50161e+08	4.50161e+08
43	5.47016e+08	6.47016e+08
44	3.10869e+08	4.10869e+08
45	658278	1.00658e+08
46	3.60167e+08	4.60167e+08
47	2.59315e+08	3.59315e+08
48	1.93434e+08	2.93434e+08
49	2.91832e+08	3.91832e+08
50	5.40168e+08	6.40168e+08